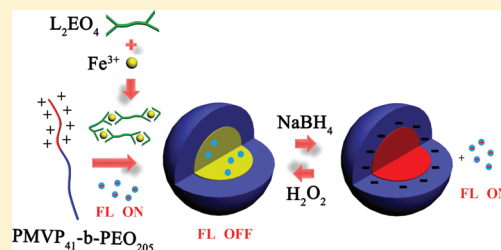


# Redox-Gated Potential Micellar Carriers Based on Electrostatic Assembly of Soft Coordination Suprapolymers

Li Zhao, Yun Yan,\* and Jianbin Huang\*

Beijing National Laboratory for Molecular Sciences (BNLMS) (State Key Laboratory for Structural Chemistry of Unstable and Stable Species), College of Chemistry and Molecular Engineering, Peking University, Beijing 100871, P. R. China

**ABSTRACT:** We report in this paper the release and uptake of charged payloads in redox responsive electrostatic micellar systems composed of negatively charged soft iron coordination suprapolymers and positively charged block copolymers. This micellar system was reported in our previous work (Yan, Y.; Lan, Y. R.; de Keizer, A.; Drechsler, M.; Van As, H.; Stuart, M. A. C.; Besseling, N. A. M. Redox responsive molecular assemblies based on metallic coordination polymers. *Soft Matter*, 2010, 6, 3244–3248), where we proposed that the system can be used as a redox-triggered release and uptake system. In this paper, we successfully selected a negatively charged fluorescent dye, eosin B, as a model cargo to track the release and upload process. Upon being compacted in the mixed micelles of coordination polymers and diblock copolymers, the fluorescence of eosin B was effectively quenched. Once reduction was conducted, excess negative charges were introduced to the mixed micelles so that the negatively charged eosin B was expelled out which was accompanied by the recovery of the fluorescence. The free negatively charged eosin B was able to be taken up by the Fe(II) micelles again if oxidation of Fe(II) was carried out since excess positive charges were produced. Beside eosin B, other charged species, such as various charged macromolecules, were tested to be capable of uptake and release by this micellar system. We suppose this system can be potentially used as a redox-gated micellar carrier for uptake and release of charged cargos.



## 1. INTRODUCTION

Electrostatic micelles have attracted considerable interest due to their potential application as carriers for functional cargos.<sup>1–3</sup> Different from conventional micelles that formed through hydrophobic interactions, these micelles are formed between oppositely charged components; thus, electrostatic interaction is the main driving force for micellization. This mechanism enables the packing of charged cargos using oppositely charged components,<sup>2</sup> and can be used as a carrier system for water-soluble molecules.<sup>4,5</sup> For instance, Lindman and co-workers,<sup>6,7</sup> and Wang and co-workers<sup>8,9</sup> have investigated compactation of DNA using electrostatic micelles. The advantage of these micellar carriers is their controllable loading amount since micelles may form at different payload to carrier molecule ratios.<sup>11,12</sup>

In the past decade, a large variety of molecules have been explored as carriers for charged cargos, such as surfactants<sup>8,13,14</sup> and block polyelectrolytes.<sup>15–17</sup> Among which, the formation of polyion complex (PIC) micelles between a pair of charged block copolymer and an oppositely charged cargos is of special interest.<sup>18</sup> The only requirement for the successful loading of target cargos in this strategy is the suitable block length of the charged block copolymers. No critical aggregation concentration is particularly emphasized because electrostatic interaction will anyway brings about formation of electrostatic micelles even at concentrations of a few ppm. Therefore, no hydrophobic section is needed in the design of this kind of carrier system.

Lately, much effort has been directed toward engineering “smart” polymeric micellar systems featuring stimuli-responsive

encapsulation and release.<sup>5,19</sup> Fabrication of redox active micelles is one of the most attractive approaches to this end.<sup>21–26</sup> The most popular design is to introduce redox sensitive groups into the polymeric chain.<sup>21,25,26</sup> Then the gate to encapsulation or release is controlled by the switch between the reduced and oxidized state of the polymers. This means that complicated lab synthesis must be done before use of these systems, which greatly restricts the broad exploration of such smart systems. Herein, we report a redox responsive system based on a smart soft coordination suprapolymer which is formed conveniently by Fe<sup>3+</sup> ions and bisligand L<sub>2</sub>EO<sub>4</sub> in aqueous solution, as demonstrated in our previous work.<sup>27</sup> We have verified that, upon addition of a block polyelectrolyte PMVP<sub>41</sub>-b-PEO<sub>205</sub> to this solution, core-shell type redox switchable micelles can be formed. The unique feature of these micelles is that the micelles keep alive before and after a redox stimulus, but the charge density shifts.<sup>27</sup> Then by utilizing electrostatic forces properly, charged cargos can be smartly uploaded or released from the core of these micelles. This was foreseen in our previous work, but by then we could not find a proper cargo to experimentally verify this because the micellar core is very small so that any change of core structure can hardly be detected microscopically. Therefore, we turned our eyes to the spectra method, and finally found a fluorescent dye eosin B that exhibits distinct fluorescence quenching after micellization. In this paper, we report the detailed experimental

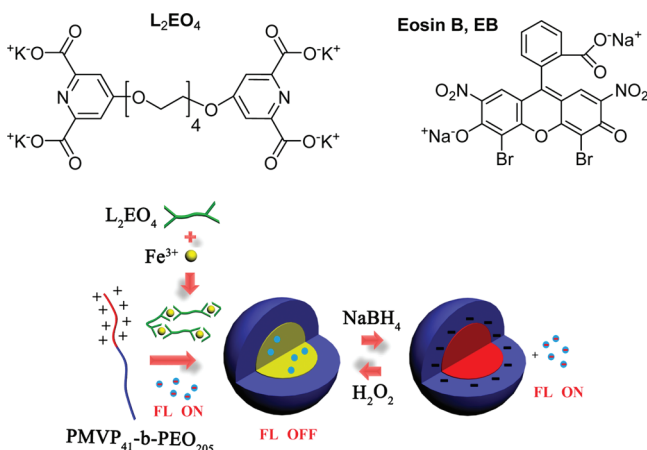
Received: December 9, 2011

Revised: March 8, 2012

Published: March 13, 2012

proof for the uptake and release of eosin B when the micelles are treated with a redox stimulus. In addition, we also found that, by analyzing the zeta potential of the particles in various cases, the system was verified to be potentially used as redox-gated nanocarrier for many charged species, as demonstrated in Scheme 1.

**Scheme 1. Illustration of the Structure of  $L_2EO_4$  (upper) and Demonstration of the Redox Triggered Uptake and Release of Fluorescent Eosin B by the Micelles<sup>a</sup>**



<sup>a</sup>Before being entrapped into micelles, eosin B shows strong fluorescence (FL) (FL ON); whereas the fluorescence is quenched after being taken up into micelles (FL OFF).

## 2. EXPERIMENTAL SECTION

**2.1. Materials.** The bisligand  $L_2EO_4$  and diblock polyelectrolyte poly(*N*-methyl-2-vinylpyridinium iodide)-*b*-poly(ethylene oxide) (PMVP<sub>41</sub>-*b*-PEO<sub>205</sub>,  $M_w = 18.5$  K, PDI = 1.05, about 90% quaternized) used in this work were prepared according to previously reported procedures.<sup>28–32</sup> Eosin B (Alfa Aesar Chemical Co. A.R.),  $FeCl_3 \cdot 6H_2O$ ,  $FeCl_2 \cdot 6H_2O$ ,  $NaBH_4$  (Beijing Chemicals Company, AR), and  $H_2O_2$  (Beijing Chemicals Company, 30%) were used without further purification.

**2.2. Sample Preparation.** Stock solutions of PMVP<sub>41</sub>-*b*-PEO<sub>205</sub>,  $L_2EO_4$ , eosin B (abbreviated as EB in the following), and  $FeCl_3$  (or  $FeCl_2$ ) were prepared at appropriate concentrations using ultrapure water. To prepare the Fe(III) coordination supramolecular complexes, 5 mM  $L_2EO_4$  solution and freshly prepared 50 mM  $FeCl_3$  (or  $FeCl_2$ ) solution were mixed at equal molar ratio. The coordination complexes and/or eosin B solutions were added in stoichiometric amounts to a PMVP<sub>41</sub>-*b*-PEO<sub>205</sub> aqueous solution ( $[+] = 1$  mM) to reach charge neutral mixing. Here,  $[+]$  stands for the molar concentration of positive charges carried by the polyelectrolyte PMVP<sub>41</sub>-*b*-PEO<sub>205</sub>. The positive charge fraction or mixing ratio is defined as  $f_+ = [ + ] / ([ + ] + [ - ])$ , with  $[ - ]$  being the molar concentration of the negative charges of the Fe(III) coordination polymers or eosin B.

**2.3. Characterization.** A Hitachi F-4500 fluorescence spectrometer was used to measure the fluorescence emission of eosin B. The excitation wavelength was set at 514 nm. Emission spectra were recorded in the range of 500–650 nm. The measuring temperature was 30 °C, and pH of solutions was controlled between 6 and 7 by adding HCl or NaOH to avoid the hydrolysis of iron. The pH values were measured using a SevenMulti type pH meter with InLab Semi-Micro electrodes (Mettler Toledo, Switzerland).

Dynamic light scattering measurements were carried out using a spectrometer of standard design (ALV-5000/E/WIN Multiple Tau Digital Correlator) with a Spectra-Physics 2017 22 mW Ar laser (wavelength: 632.8 nm). The temperature was controlled at  $30 \pm 0.5$

°C using a Haake C35 thermostat. To prepare dust-free solutions for light scattering measurements, the solutions were filtered through a 0.22  $\mu m$  membrane of hydrophilic PVDF filter into light scattering cells before the measurements. The scattering angle was 90°, and the intensity autocorrelation functions were analyzed by using the method of CONTIN.

A JEM-2100 instrument was employed to observe the morphology of micelles. Drops of samples were put on to 230 mesh copper grids coated with ultrathin carbon film. Excess water was removed by filter paper and samples were then allowed dry in ambient air at room temperature, before transmission electron microscopy (TEM) observation.

X-ray photoelectron spectroscopy (XPS) measurements were carried out on an AXIS-Ultra instrument from Kratos Analytical using monochromatic Al  $K\alpha$  radiation (225 W, 15 mA, 15 kV) and low-energy electron flooding for charge compensation. Target PIC micelle solutions were dropped onto a clean silicon wafer, followed by drying naturally. To compensate for surface charge effects, binding energies were calibrated using the C 1s hydrocarbon peak at 284.80 eV. The data were converted into VAMAS file format and imported into CasaXPS software package for manipulation and curve-fitting.

Zeta potentials were measured using a temperature-controlled ZetaPALS zeta potential analyzer (Brookhaven Instruments Corporation).

## 3. RESULTS AND DISCUSSION

Iron-containing PIC micelles were easily obtained in the mixed aqueous solution of iron,  $L_2EO_4$ , and a block polyelectrolyte PMVP<sub>41</sub>-PEO<sub>205</sub> as reported in our previous work,<sup>27</sup> where iron and  $L_2EO_4$  form negatively charged soft coordination polymers. Then, like other PIC systems, these negatively charged coordination polymers interact with the positively charged PMVP<sub>41</sub> block of MVP<sub>41</sub>-PEO<sub>205</sub> to form PIC micelles. The micelles were found to exist in a wide range of charge ratios, ranging from  $f_- = 0.25$ –0.8 for Fe(III) and 0.35–0.8 for Fe(II) ( $f_-$  is the molar fraction of the negative charges over the summation of the positive and negative charges on the polymers).<sup>33</sup> This wide micellar formation range enables both micelles to keep alive after a redox stimulus.<sup>27</sup>

**3.1. Qualification of Cargoes.** Before conducting reduce-triggered release of payload in the Fe(III) micellar system, we tried to find a proper cargo for this study. In principle, the target cargo can be a wide category of negatively charged molecules or nanometer-sized particles. However, for the convenience of characterization, here we have to choose a negatively charged one that has significant response to micellization with PMVP<sub>41</sub>-PEO<sub>205</sub> while being inert to Fe(III)- $L_2EO_4$ . After delicate selection, we focused on a negatively charged dye, eosin B, which is fluorescent in aqueous media and the fluorescence is not affected by the presence of iron coordination polymers but can be effectively quenched by PMVP<sub>41</sub>-PEO<sub>205</sub>. This is because the eosin B carries charges of the same sign as coordination polymers but also opposite to the charges of the PMVP<sub>41</sub> block. As a result, the local concentration of eosin B can be enhanced in the presence of PMVP<sub>41</sub>-PEO<sub>205</sub> which results in self-quenching (Figure 1). It can be seen from the inset in Figure 1 that the fluorescence intensity decreases almost linearly with increasing the charge ratio of eosin B to that of the PMVP<sub>41</sub>-PEO<sub>205</sub>, suggesting that any electrostatic complexation of eosin B with PMVP<sub>41</sub>-PEO<sub>205</sub> leads to quenching of fluorescence. This means that by measuring the fluorescence intensity we can conveniently know whether the dyes are released or taken up by the micelles.

Next, the micellization abilities of eosin B/PMVP<sub>41</sub>-PEO<sub>205</sub> and Fe(III)- $L_2EO_4$ /PMVP<sub>41</sub>-PEO<sub>205</sub> were compared. We

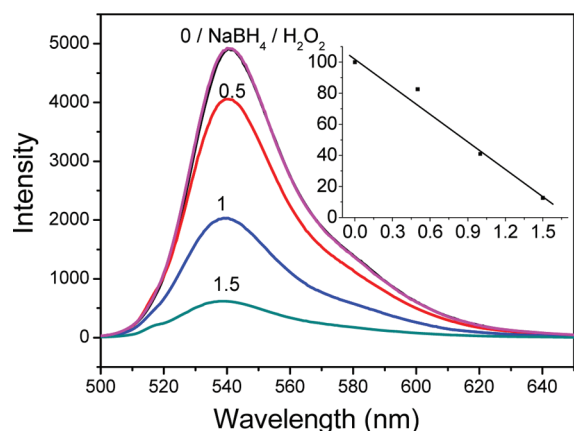


**Figure 1.** Influence of coordination polymer Fe(III)–L<sub>2</sub>EO<sub>4</sub>, block polyelectrolyte PMVP<sub>41</sub>–PEO<sub>205</sub> on the fluorescence intensity of 0.02 mM eosin B. NaBH<sub>4</sub> or H<sub>2</sub>O<sub>2</sub> shows no influence on the fluorescence of eosin B, which will be mentioned in section 3.2, and for reference in section 3.3. The numbers on the top of each curve are the molar charge ratio between eosin B and PMVP<sub>41</sub>–PEO<sub>205</sub>. The inset shows the linear decrease of fluorescence with increasing eosin B to PMVP<sub>41</sub>–PEO<sub>205</sub> charge ratio.

first prepared the mixed micelles between eosin B, Fe(III)–L<sub>2</sub>EO<sub>4</sub>, and PMVP<sub>41</sub>–PEO<sub>205</sub> at charge-neutral mixing ratio, where the summation of the negative charge concentration of eosin B and Fe(III)–L<sub>2</sub>EO<sub>4</sub> is equal to the overall positive charges provided by PMVP<sub>41</sub>–PEO<sub>205</sub>. Dynamic light scattering (DLS) results (Figure 2) clearly demonstrate that well-defined

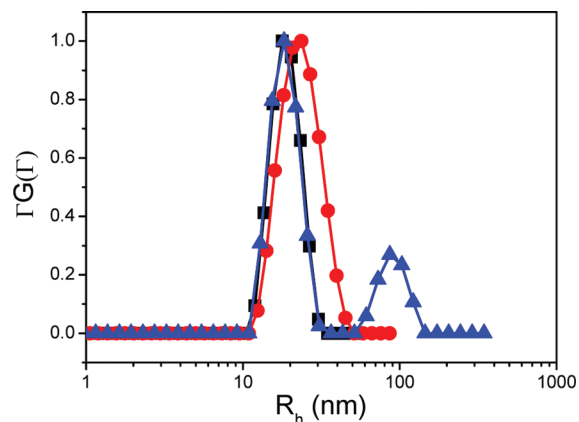


**Figure 2.** Comparison of micelles formed between eosin B or Fe(III)–L<sub>2</sub>EO<sub>4</sub> and PMVP<sub>41</sub>–PEO<sub>205</sub>. For Fe(III)–L<sub>2</sub>EO<sub>4</sub>/PMVP<sub>41</sub>–PEO<sub>205</sub> mixed micelles (■), [Fe(III)–L<sub>2</sub>EO<sub>4</sub>] = [PMVP<sub>41</sub>–PEO<sub>205</sub>] = 0.67 mM; eosin/PMVP<sub>41</sub>–PEO<sub>205</sub> mixed micelles (▲), [eosin B] = [PMVP<sub>41</sub>–PEO<sub>205</sub>] = 0.67 mM; Fe(III)–L<sub>2</sub>EO<sub>4</sub>/eosin B/PMVP<sub>41</sub>–PEO<sub>205</sub> mixed micelles (●), [Fe(III)–L<sub>2</sub>EO<sub>4</sub>] = [eosin B] = 0.335 mM, [PMVP<sub>41</sub>–PEO<sub>205</sub>] = 0.67 mM.

micelles with an average hydrodynamic radius of 23 nm were formed. This size is larger than that of the micelles formed by directly mixing Fe(III)–L<sub>2</sub>EO<sub>4</sub> and PMVP<sub>41</sub>–PEO<sub>205</sub> (18 nm), and is also different from that of the mixed micelles formed by eosin B and PMVP<sub>41</sub>–PEO<sub>205</sub>. In the latter case, two groups of colloidal particles were formed: one is of the same hydrodynamic radius of 18 nm, and the other is about 86 nm. Upon comparison with micelles in the Fe(III)–L<sub>2</sub>EO<sub>4</sub> /PMVP<sub>41</sub>–PEO<sub>205</sub> system, the 18 nm particles can be attributed to micelles formed by Fe(III)–L<sub>2</sub>EO<sub>4</sub> and PMVP<sub>41</sub>–PEO<sub>205</sub>,

whereas the particles at 86 nm are loose clusters of eosin B/PMVP<sub>41</sub>–PEO<sub>205</sub> complexes. The presence of these loose clusters suggests a weaker interaction between EB and PMVP<sub>41</sub>–PEO<sub>205</sub> than that between Fe(III)–L<sub>2</sub>EO<sub>4</sub> and PMVP<sub>41</sub>–PEO<sub>205</sub>. Figure 3 shows that the loose cluster appears

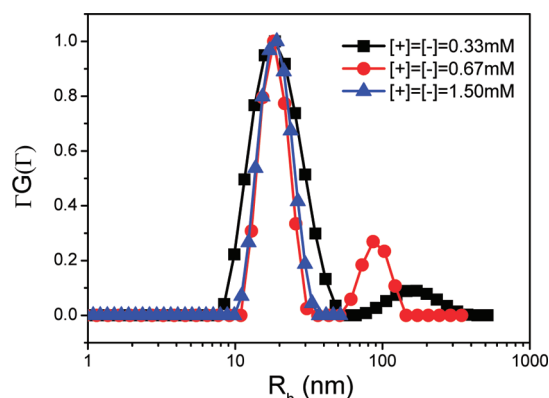


**Figure 3.** Formation of mixed micelles between eosin B and PMVP<sub>41</sub>–PEO<sub>205</sub> at different concentrations. Loose clusters appear at concentration lower than 0.67 mM.

only at charge concentration below 0.67 mM, indicating that well-defined micelles are formed at concentrations beyond a critical value, which is common in such micellar systems.<sup>34</sup> This weaker interaction is also reflected in the larger size of eosin B/Fe(III)–L<sub>2</sub>EO<sub>4</sub>/PMVP<sub>41</sub>–PEO<sub>205</sub> mixed PIC micelles, which leads to an increase of the micellar size from 18 to 23 nm.

It is well-known that charge density matching between the oppositely charged block plays a very important role in the formation of stable micelles.<sup>35</sup> For covalent polyelectrolyte systems, it is often that not well-defined micelles, but loose clusters, can be formed if the charge density is considerably mismatched.<sup>36</sup> In mixed systems that can form micelles, the interaction between charge-matched pairs is much stronger than those mismatched ones. This is also the case in the eosin B/Fe(III)–L<sub>2</sub>EO<sub>4</sub>/PMVP<sub>41</sub>–PEO<sub>205</sub> mixed micellar system. Since the size of Fe(III)–L<sub>2</sub>EO<sub>4</sub> matches the PMVP block of PMVP<sub>41</sub>–PEO<sub>205</sub> better than that of eosin B, PMVP<sub>41</sub>–PEO<sub>205</sub> favors complexation with Fe(III)–L<sub>2</sub>EO<sub>4</sub> so that eosin B has to be released from the mixed micelles upon addition of Fe(III)–L<sub>2</sub>EO<sub>4</sub>. This release of eosin B can be recognized from the recovery of the fluorescence, since we have verified in Figure 1 that any form of complexation of eosin B with PMVP<sub>41</sub>–PEO<sub>205</sub> leads to significant fluorescence quenching. As demonstrated in Figure 4, the fluorescence intensity indeed recovers gradually with increasing the amount of Fe(III)–L<sub>2</sub>EO<sub>4</sub> in the eosin B/PMVP<sub>41</sub>–PEO<sub>205</sub> mixed systems, suggesting successful release of eosin B from the micelles.

**3.2. Reduction-Triggered Release of Eosin B.** The preferable binding of Fe(III)–L<sub>2</sub>EO<sub>4</sub> with PMVP<sub>41</sub>–PEO<sub>205</sub> allows us to perform reduction-triggered release of eosin B from the mixed micelles of eosin B/Fe(III)–L<sub>2</sub>EO<sub>4</sub>/PMVP<sub>41</sub>–PEO<sub>205</sub> at charge neutral mixing ratio. It is known that, after reduction, the elementary charges at every coordination center of Fe(III)–L<sub>2</sub>EO<sub>4</sub> increase from –1 to –2, as demonstrated in Scheme 2. This means that there will be excess negative charges in the micelles after reduction. Therefore, the micelles have to expel out some negative species, either eosin B or Fe(III)–L<sub>2</sub>EO<sub>4</sub>. According to the results in the previous text (Figure 4), we expect that eosin B will be released from the micelles due to

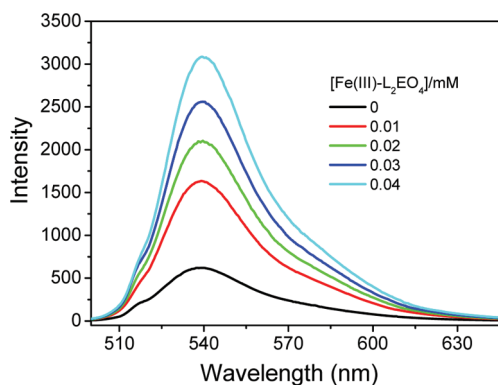
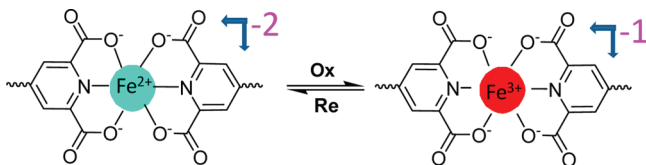


**Figure 4.** Recovery of the eosin B fluorescence upon expelling eosin B from the 0.02 mM eosin B/0.03 mM PMVP<sub>41</sub>-PEO<sub>205</sub> mixed micelles with addition of Fe(III)-L<sub>2</sub>EO<sub>4</sub>.

### Scheme 2. Illustration of the Change of the Charge Density in a Coordination Center after a Redox Stimulus



it is weaker interaction with PMVP<sub>41</sub>-PEO<sub>205</sub>. If this occurs, an increase of the fluorescence intensity will be observed. This is indeed the case. As demonstrated in Figure 5, with increasing

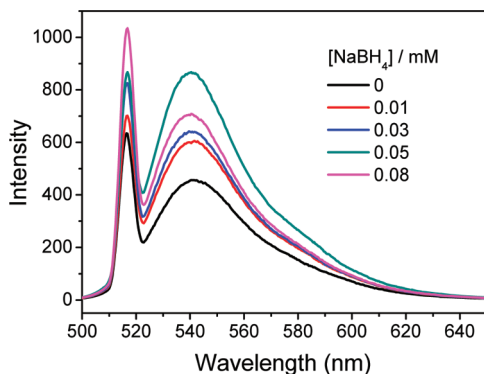


**Figure 5.** Recovery of eosin B fluorescence upon reducing the micelles with NaBH<sub>4</sub>. The original micelles were formed by 0.02 mM eosin B/0.15 mM Fe(III)-L<sub>2</sub>EO<sub>4</sub>/0.30 mM PMVP<sub>41</sub>-PEO<sub>205</sub>. The spectra demonstrate the variation of fluorescence intensity with increasing the amount of NaBH<sub>4</sub>.

the amount of a reducing agent NaBH<sub>4</sub> in the mixed micellar systems of eosin B/Fe(III)-L<sub>2</sub>EO<sub>4</sub>/PMVP<sub>41</sub>-PEO<sub>205</sub>, the fluorescence of eosin B increases gradually. Since NaBH<sub>4</sub> has no effect on the fluorescence intensity of eosin B whereas PMVP<sub>41</sub>-PEO<sub>205</sub> quenches it significantly (Figure 1), this verified that reduction-triggered release of cargos from the micelles indeed occurred.

The reduction-triggered release of eosin B from the micelles is also reflected in changes in dynamic light scattering of the system. It can be found from Figure 6 that, before reduction, well-defined micelles with average hydrodynamic radius about 18 nm were formed; however, after reduction, micelles of this

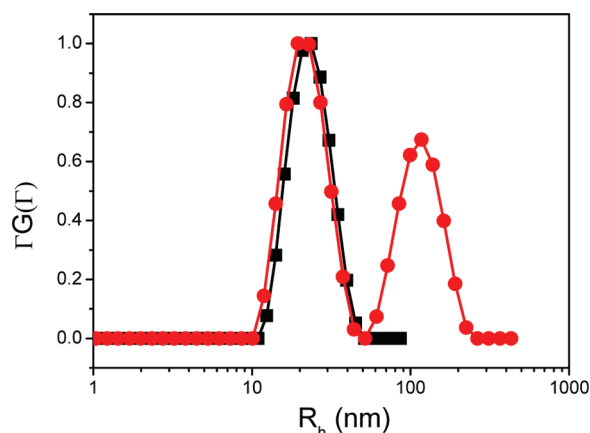


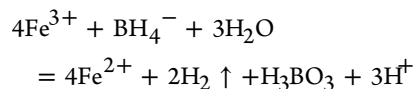
**Figure 6.** Comparison of the size of micelles before (■) and after (●) reduction with 2 mM NaBH<sub>4</sub>. The concentration of positive charges is 0.67 mM, where the overall concentration of negative charges is 0.67 mM as well. [Fe(III)-L<sub>2</sub>EO<sub>4</sub>] = [eosin B] = 0.335 mM.

size are still there, but a new family of micelles with average hydrodynamic radius around 100 nm occurs.

Since the binding between eosin B and PMVP<sub>41</sub>-PEO<sub>205</sub> is much weaker than that between Fe(III)-L<sub>2</sub>EO<sub>4</sub> and PMVP<sub>41</sub>-PEO<sub>205</sub>, the larger micelles are probably loose clusters involving eosin B. This can be verified by TEM observations (Figure 7) for the micelles with varying molar ratios of eosin B: Fe(III)-L<sub>2</sub>EO<sub>4</sub>. As can be found in Figure 7a and b, at [eosin B]/[Fe(III)-L<sub>2</sub>EO<sub>4</sub>] less than 1:1, well-defined micelles can be formed, whereas the size of the micelle slightly swells, which is in agreement with DLS measurements. However, at the [eosin B]/[Fe(III)-L<sub>2</sub>EO<sub>4</sub>] beyond 1:1 (Figure 7c), the micelles become ill-defined and loose clusters with unclear boundaries appear. The formation of loose clusters also explains the lower fluorescence intensity after reduction: the fluorescence of eosin B was quenched in the clusters so that it cannot recover to its original strength.

To further verify that Fe<sup>3+</sup> in the Fe(III)-L<sub>2</sub>EO<sub>4</sub> was reduced to Fe<sup>2+</sup>, rather than iron nanoparticles, we compared the XPS spectra of the micelles before and after reduction. In the presence of excess NaBH<sub>4</sub>, only the characteristic peak of Fe<sup>2+</sup> was observed, suggesting that the Fe<sup>3+</sup> was indeed successfully reduced into Fe<sup>2+</sup> (Figure 8).<sup>37–40</sup>

It is well-known that NaBH<sub>4</sub> often reduces Fe<sup>3+</sup> directly into Fe owing to its strong reducing ability. However, the chelating interaction increases the redox potential of metal ions, which makes it difficult to be reduced. We found in cyclic voltammetry experiments that the half-wave potential of Fe<sup>3+</sup> on a glassy carbon surface was enhanced by about 0.2 V after formation of Fe(III)-L<sub>2</sub>EO<sub>4</sub> with L<sub>2</sub>EO<sub>4</sub>. Therefore, we may confirm that the following reaction occurred when the original Fe(III) micelles were stimulated with NaBH<sub>4</sub>:



**3.3. Oxidation-Triggered Uptake of EB.** The formation of Fe<sup>2+</sup> after reduction enables our micellar system mutual switch between the oxidation and reduction state. Therefore, it can be expected that the free eosin B can be taken up into micelles if oxidant was added to the system. This indeed occurs. Figure 9 shows that after addition of H<sub>2</sub>O<sub>2</sub> to the Fe(II) micellar system that contains free eosin B, the fluorescence

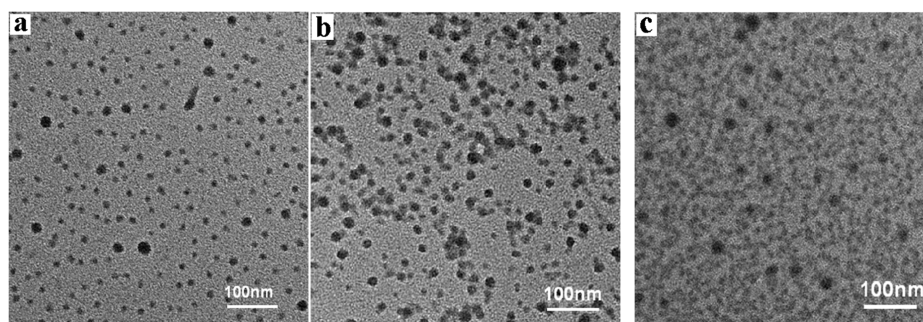


**Figure 7.** Micelles formed in eosin B/Fe(III)-L<sub>2</sub>EO<sub>4</sub>/PMVP<sub>41</sub>-PEO<sub>205</sub> mixed systems. In all the samples, the charge concentration of PMVP<sub>41</sub>-PEO<sub>205</sub> [ + ] equals to that of the summation of negative charges [ - ] from eosin B and Fe(III)-L<sub>2</sub>EO<sub>4</sub> to be 0.67 mM, whereas the molar ratio for (a–c) are [ - ]<sub>eosin B</sub>/[ - ]<sub>Fe(III)-L<sub>2</sub>EO<sub>4</sub></sub> = (a) 1:2, (b) 1:1, and (c) 2:1.

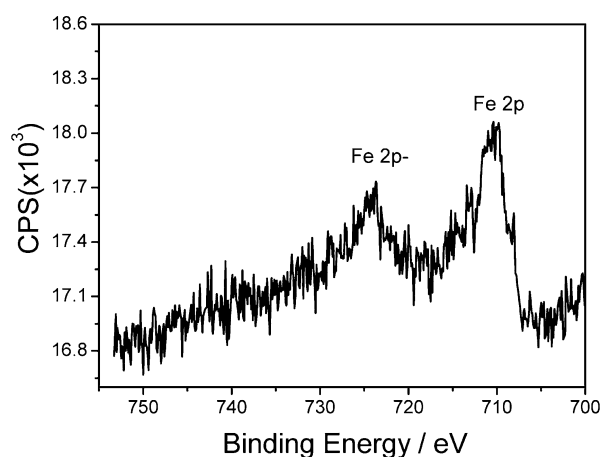


**Figure 8.** Fe 2p XPS spectrum of 0.335 mM Fe(III)-L<sub>2</sub>EO<sub>4</sub>/0.335 mM EB/0.67 mM PMVP<sub>41</sub>-PEO<sub>205</sub> micelles after reduction with 2 mM NaBH<sub>4</sub>.

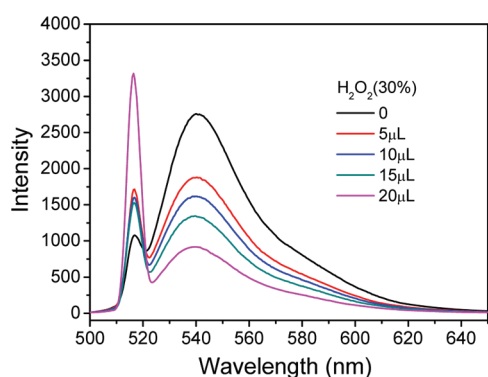


**Figure 9.** Oxidation-triggered fluorescence quenching of eosin B. The original micelles are 0.30 mM, where the negative charges from Fe(III)-L<sub>2</sub>EO<sub>4</sub> are 0.30 mM and the positive charges from PMVP<sub>41</sub>-PEO<sub>205</sub> are 0.30 mM. The concentration of eosin B is 0.02 mM.

gradually decreases, suggesting encapsulation of eosin B into the micelles. Meanwhile, a scattering peak appears at 518 nm, which indicates that more colloidal particles were formed in the process of uptake of eosin B. According to our previous result, it is believed that loose eosin B/PMVP<sub>41</sub>-PEO<sub>205</sub> clusters with larger hydrodynamic were formed besides the original iron micelles. Since the eosin B/PMVP<sub>41</sub>-PEO<sub>205</sub> clusters are larger than the Fe(III)-L<sub>2</sub>EO<sub>4</sub>/PMVP<sub>41</sub>-PEO<sub>205</sub> micelles, strong scattering of light occurs during measurement of fluorescence, which is in accordance with the lowering of fluorescence

intensity of eosin B in the process of oxidation. The peak at 518 nm is caused by particle scattering and can also be verified by measuring the fluorescence of a micellar solution without eosin. We found that this peak was observed as well when solely a Fe(III)-L<sub>2</sub>EO<sub>4</sub>/PMVP<sub>41</sub>-PEO<sub>205</sub> micellar solution was measured.

### 3.4. Generality of Redox Gated Uptake and Release.

In section 2 and 3, we have demonstrated that eosin B can be used as a model cargo that may trace the occurrence of uptake and release of materials from the micelles formed by Fe(III/II)-L<sub>2</sub>EO<sub>4</sub> and PMVP<sub>41</sub>-PEO<sub>205</sub> upon a redox stimulus. Herein we are to verify that this is a general behavior of this micellar system. To do this, we examined the variation of the zeta potential of micelles after a redox treatment. It can be found that the starting charge neutral micelles have a very small potential that is below 1 mV. However, upon reduction of the Fe(III) micelles and oxidation of the Fe(II) micelles, the potentials become more negative and positive, respectively. This is attributed to the developed excess negative or positive charges in the cores of the two micelles. These excess charges can be used to sequester any oppositely charged materials in their neighborhood. For instance, upon addition of positively charged PEI (polyethyleneimine) to the NaBH<sub>4</sub> treated Fe(III) micelles, the negative potential drops back to around zero, whereas the addition of PSS (sodium polystyrene sulfonate) to the H<sub>2</sub>O<sub>2</sub> treated Fe(II) micelles leads to a decrease of the positive potential to around zero, too (Figure 10). Although this is a very small change, it provides proof for the appearance of excess negative charges. The fact that one does not observe a significant zeta potential is because of the presence of a thick PEO corona outside the micellar core, which would bury most of the mobile countercharges.<sup>41</sup> Actually, other charged molecules may have the same effect on the potential changes for an oppositely charged micellar system given that the charge density of the molecules is larger enough.<sup>42</sup> So far, we have confirmed that the electrostatic micelles containing iron coordination polymers can indeed serve as a redox gated uptake and release system.

## 4. CONCLUSIONS

In summary, we have verified the possibility of uptake and release of charged cargos in redox responsive electrostatic micellar systems using a fluorescent dye eosin B as the model cargo. The micelles were formed by a negatively charged soft iron coordination suprapolymer and a positively charged block copolymer via electrostatic interaction at charge neutral mixing ratio. Upon redox treatment, the micelles may acquire excess

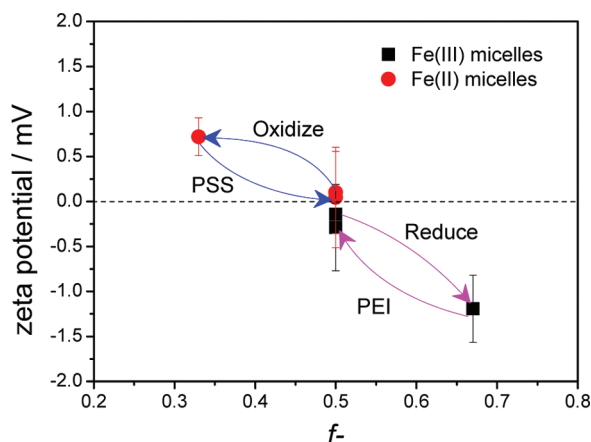


**Figure 10.** Variation of zeta potentials of Fe(III) micelles (■) and Fe(II) micelles (●) with the reduction/oxidation and the addition of PEI/PSS, respectively. The original charge concentration of Fe(III) micelles and Fe(II) micelles was 1 mM.  $[\text{NaBH}_4] = 2 \text{ mM}$ ,  $[\text{H}_2\text{O}_2] = 3 \mu\text{L}$ ,  $[\text{PEI}] = [\text{PSS}] = 1 \text{ mM}$ .

positive or negative charges depending on the starting oxidation state of iron. Thus, the negatively charged eosin B can be repelled out or taken up into the micelles, as was reflected by the change of the fluorescence intensity of eosin B. The fluorescence was quenched after uptake, whereas it was increased after release. This redox controlled uptake and release can be generalized to other charged materials, where the encapsulation of oppositely charged materials into the charged micelles leads to a decrease of the potential. During redox switches, the iron-containing micelles do not disintegrate so that we expect that this system can be potentially used as “micellar carriers” to ship cargos.

## AUTHOR INFORMATION

### Corresponding Author

\*Telephone: +86 10 62765058. Fax: +86 10 62765058. E-mail: yunyan@pku.edu.cn (Y.Y.); jbhuan@pku.edu.cn (J.H.).

### Notes

The authors declare no competing financial interest.

## ACKNOWLEDGMENTS

This research was supported by National Natural Science Foundation of China (20903005, 21173011, 21073006, and 51121091).

## REFERENCES

- Voets, I. K.; de Keizer, A.; Stuart, M. A. C. Complex coacervate core micelles. *Adv. Colloid Interface Sci.* **2009**, *147–48*, 300–318.
- Lee, Y.; Fukushima, S.; Bae, Y.; Hiki, S.; Ishii, T.; Kataoka, K. A protein nanocarrier from charge-conversion polymer in response to endosomal pH. *J. Am. Chem. Soc.* **2007**, *129*, 5362–5363.
- Osada, K.; Kataoka, K. Drug and gene delivery based on supramolecular assembly of PEG-polypeptide hybrid block copolymers. *Adv. Polym. Sci.* **2006**, *202*, 113–153.
- Shiraishi, K.; Kawano, K.; Maitani, Y.; Yokoyama, M. Polyion complex micelle MRI contrast agents from poly(ethylene glycol)-*b*-poly(L-lysine) block copolymers having Gd-DOTA; preparations and their control of T(1)-relaxivities and blood circulation characteristics. *J. Controlled Release* **2010**, *148*, 160–167.
- Zhang, G. D.; Harada, A.; Nishiyama, N.; Jiang, D. L.; Koyama, H.; Aida, T.; Kataoka, K. Polyion complex micelles entrapping cationic dendrimer porphyrin: effective photosensitizer for photodynamic therapy of cancer. *J. Controlled Release* **2003**, *93*, 141–150.

- Gaweda, S.; Pais, A. A. C. C.; Dias, R. S.; Schillen, K.; Lindman, B.; Miguel, M. G.; Moran, M. C. Cationic agents for DNA compaction. *J. Colloid Interface Sci.* **2008**, *323*, 75–83.

- Gonzalez-Perez, A.; Alatorre-Meda, M.; Dias, R. S.; Lindman, B.; Carlstedt, J. Release of DNA from surfactant complexes induced by 2-hydroxypropyl-beta-cyclodextrin. *Int. J. Biol. Macromol.* **2010**, *46*, 153–158.

- Cao, M. W.; Deng, M. L.; Wang, X. L.; Wang, Y. L. Decompaction of Cationic Gemini Surfactant-Induced DNA Condensates by beta-Cyclodextrin or Anionic Surfactant. *J. Phys. Chem. B* **2008**, *112*, 13648–13654.

- Wang, X. L.; Zhang, X. H.; Cao, M. W.; Zheng, H. Z.; Xiao, B.; Wang, Y. L.; Li, M. Gemini Surfactant-Induced DNA Condensation into a Beadlike Structure. *J. Phys. Chem. B* **2009**, *113*, 2328–2332.

- Willerich, I.; Schindler, T.; Ritter, H.; Grohn, F. Controlling the size of electrostatically self-assembled nanoparticles with cyclodextrin as external trigger. *Soft Matter* **2011**, *7*, 5444–5450.

- Willerich, I.; Li, Y.; Grohn, F. Influencing Particle Size and Stability of Ionic Dendrimer-Dye Assemblies. *J. Phys. Chem. B* **2010**, *114*, 15466–15476.

- Willerich, I.; Grohn, F. Photoswitchable Nanoassemblies by Electrostatic Self-Assembly. *Angew. Chem., Int. Ed.* **2010**, *49*, 8104–8108.

- Dias, R.; Miguel, M. D.; Lindman, B.; Rosa, M. DNA-cationic surfactant interactions are different for double- and single-stranded DNA. *Biomacromolecules* **2005**, *6*, 2164–2171.

- Schillen, K.; Nylander, T.; Jansson, J.; Lindman, B.; Cardenas, M. DNA compaction by cationic surfactant in solution and at polystyrene particle solution interfaces: a dynamic light scattering study. *Phys. Chem. Chem. Phys.* **2004**, *6*, 1603–1607.

- Lee, Y.; Kataoka, K. Biosignal-sensitive polyion complex micelles for the delivery of biopharmaceuticals. *Soft Matter* **2009**, *5*, 3810–3817.

- Kataoka, K.; Nagasaki, Y.; Oishi, M. pH-responsive three-layered PEGylated polyplex micelle based on a lactosylated ABC triblock copolymer as a targetable and endosome-disruptive nonviral gene vector. *Bioconjugate Chem.* **2006**, *17*, 677–688.

- Oh, K. T.; Bronich, T. K.; Bromberg, L.; Hatton, T. A.; Kabanov, A. V. Block ionomer complexes as prospective nanocontainers for drug delivery. *J. Controlled Release* **2006**, *115*, 9–17.

- Yamauchi, K.; Harada, A.; Takamisawa, I.; Shimokado, K.; Kataoka, K.; Harada-Shiba, M. Polyion complex micelles as vectors in gene therapy - pharmacokinetics and in vivo gene transfer. *Gene Ther.* **2002**, *9*, 407–414.

- Nagatsugi, F.; Sasaki, S.; Nagasaki, Y.; Kataoka, K.; Oishi, M. Smart polyion complex micelles for targeted intracellular delivery of PEGylated antisense oligonucleotides containing acid-labile linkages. *ChemBioChem* **2005**, *6*, 718–725.

- MacEwan, S. R.; Callahan, D. J.; Chilkoti, A. Stimulus-responsive macromolecules and nanoparticles for cancer drug delivery. *Nanomedicine (London, U.K.)* **2010**, *5*, 793–806.

- Ryu, J. H.; Roy, R.; Ventura, J.; Thayumanavan, S. Redox-Sensitive Disassembly of Amphiphilic Copolymer Based Micelles. *Langmuir* **2010**, *26*, 7086–7092.

- Bigot, J.; Charleux, B.; Delattre, F.; Fournier, D.; Lyskawa, J.; Sambe, L.; Stoffelbach, F.; Woisel, P.; Cooke, G. Tetrathiafulvalene End-Functionalized Poly(N-isopropylacrylamide): A New Class of Amphiphilic Polymer for the Creation of Multistimuli Responsive Micelles. *J. Am. Chem. Soc.* **2010**, *132*, 10796–10801.

- Hoshino, K.; Aoyagui, S.; Saji, T. Reversible formation and disruption of micelles by control of the redox state of the head group. *J. Am. Chem. Soc.* **1985**, *107*, 6865–6868.

- Ryu, J. H.; Chacko, R. T.; Jiwanich, S.; Bickerton, S.; Babu, R. P.; Thayumanavan, S. Self-Cross-Linked Polymer Nanogels: A Versatile Nanoscopic Drug Delivery Platform. *J. Am. Chem. Soc.* **2010**, *132*, 17227–17235.

- Ma, N.; Li, Y.; Xu, H. P.; Wang, Z. Q.; Zhang, X. Dual Redox Responsive Assemblies Formed from Diselenide Block Copolymers. *J. Am. Chem. Soc.* **2010**, *132*, 442–443.

(26) Kim, H.; Jeong, S. M.; Park, J. W. Electrical Switching between Vesicles and Micelles via Redox-Responsive Self-Assembly of Amphiphilic Rod-Coils. *J. Am. Chem. Soc.* **2011**, *133*, 5206–5209.

(27) Yan, Y.; Lan, Y. R.; de Keizer, A.; Drechsler, M.; Van As, H.; Stuart, M. A. C.; Besseling, N. A. M. Redox responsive molecular assemblies based on metallic coordination polymers. *Soft Matter* **2010**, *6*, 3244–3248.

(28) Yan, Y.; Besseling, N. A. M.; de Keizer, A.; Marcelis, A. T. M.; Drechsler, M.; Stuart, M. A. C. Hierarchical self-organization in solutions containing metal ions, ligand, and diblock copolymer. *Angew. Chem., Int. Ed.* **2007**, *46*, 1807–1809.

(29) Yan, Y.; Martens, A. A.; Besseling, N. A. M.; de Wolf, F. A.; de Keizer, A.; Drechsler, M.; Cohen Stuart, M. A. Nanoribbons Self-assembled from Triblock Peptide Polymers and Coordination Polymers. *Angew. Chem., Int. Ed.* **2008**, *47*, 4192–4195.

(30) Yan, Y.; Harnau, L.; Besseling, N. A. M.; de Keizer, A.; Ballauff, M.; Rosenfeldt, S.; Cohen Stuart, M. A. Spherocylindrical Coacervate Core Micelles formed by a Supramolecular Coordination Polymer and a Diblock Copolymer. *Soft Matter* **2008**, *4*, 2207–2212.

(31) Yan, Y.; Besseling, N. A. M.; de Keizer, A.; Cohen Stuart, M. A. Characteristic Differences in the Formation of Complex Coacervate Core micelles from Neodymium and Zinc Based Coordination Polymers. *J. Phys. Chem. B* **2007**, *111*, 5811–5818.

(32) Wang, J. Y.; de Keizer, A.; Van Leeuwen, H. P.; Yan, Y.; Vergeldt, F.; van As, H.; Bomans, P. H. H.; Sommerdijk, N. A. J.; Cohen Stuart, M. A.; van der Gucht, J. Effect of pH on Complex Coacervate Core Micelles from Fe(III)-Based Coordination Polymer. *Langmuir* **2011**, *27*, 14776–14782.

(33) Wang, J. Y.; de Keizer, A.; Fokkink, R.; Yan, Y.; Stuart, M. A. C.; van der Gucht, J. Complex Coacervate Core Micelles from Iron-Based Coordination Polymers. *J. Phys. Chem. B* **2010**, *114*, 8313–8319.

(34) Yan, Y.; de Keizer, A.; Stuart, M. A. C.; Drechsler, M.; Besseling, N. A. M. Stability of Complex Coacervate Core micelles Containing Metal Coordination Polymer. *J. Phys. Chem. B* **2008**, *112*, 10908–10914.

(35) Harada, A.; Kataoka, K. Core-shell supramolecular assembly from oppositely charged block copolymers. *Science* **1999**, *283*, 65–67.

(36) van der Burgh, S.; de Keizer, A.; Stuart, M. A. C. Complex coacervation core micelles: Colloidal stability and aggregation mechanism. *Langmuir* **2004**, *20*, 1073–1084.

(37) Welsh, I. D.; Sherwood, P. M. A. M. Photoemission and Electronic Structure of FeOOH: Distinguishing Between Oxide and Oxyhydroxide. *Phys. Rev. B* **1989**, *40*, 6386–6392.

(38) Fujii, T.; de Groot, F. M. F.; Sawatzky, G. A.; Voogt, F. C.; Hibma, T.; Okada, K. In situ XPS analysis of various iron oxide films grown by NO<sub>2</sub>-assisted molecular-beam epitaxy. *Phys. Rev. B* **1999**, *59*, 3195–3202.

(39) McIntyre, N. S.; Zetaruk, D. G. X-ray photoelectron spectroscopic studies of iron oxides. *Anal. Chem.* **1977**, *49*, 1521–1529.

(40) Harvey, D. T.; Linton, R. W. Chemical characterization of hydrous ferric oxides by x-ray photoelectron spectroscopy. *Anal. Chem.* **1981**, *53*, 1684–1688.

(41) Yan, Y.; de Keizer, A.; Stuart, M. A. C.; Drechsler, M.; Besseling, N. A. M. Capacity controllable nanocarriers for metal ions. *Soft Matter* **2009**, *5*, 790–796.

(42) Ding, Y.; Yang, Y.; Yang, L.; Yan, Y.; Huang, J. B.; Stuart, M. A. C. A case of adaptive self-assembly. *ACS Nano* **2012**, *6*, 1004–1010.